*Sādhanā* (2022) 47:75
https://doi.org/10.1007/s12046-022-01852-z


# Performance enhancement in WEDM of nitronic-30 using latent heat energy

NILESH T MOHITE[1,*], GEETANJALI V PATIL[1] and ANUPAMA N KALLOL[2]

[1]Bijapur Liberal District Educational Assocation (BLDEA's) Vachana Pitamaha (VP). Dr. Phakirappa Gurubasappa Halakatti College of Engineering and Technology, 586101 Vijaypur, India
[2]Department of Mechanical Engineering, KLS Gogte Institute of Technology, Belagavi, Karnataka 590008, India
e-mail: nilesh.242933@gmail.com

MS received 31 October 2020; revised 11 February 2022; accepted 24 February 2022

**Abstract.** In the present study, finite element thermal modeling of wire electrical discharge machining (WEDM) process for Nitronic-30 has been done. The modeling has been done by considering important aspects such as energy distribution factor, Gaussian heat distribution and latent heat of fusion to predict thermal behavior as well as material removal mechanism in WEDM process. The Temperature distribution on the work piece has been computed using ANSYS software and temperature distribution profiles obtained are used to determine the theoretical MRR. Validation of model MRR with experimental MRR shows very good agreement.

**Keywords.** WEDM; MRR; ANSYS; Latent heat of fusion.

## 1. Introduction

Due to advancement in technology, the manufacturing industry is demanding for high precision machining processes. Similarly, complex shapes of components require machining with high precision.

WEDM is most commonly used nontraditional machining process as it is able to produce complex shapes. Conductive materials can be easily machined by WEDM due to the fact that work piece material and wire electrode do not have mechanical contact. This makes WEDM process ideal and unique [1].

WEDM finds use in areas like nuclear, automotive and manufacturing industry because of excellent machining abilities. From the beginning of WEDM, the research is continuously going on for the sake of improvement in the performance of WEDM process. Performing experiments on WEDM is time consuming and costly as well. Therefore, to study the behavior of this process, it is essential to consider different machining parameters, use of modeling and simulation software.

In the present paper, efforts have been made to develop a thermal model for WEDM using ANSYS software by incorporating the effect of latent heat of fusion or phase change, calculating exact value of amount of energy absorbed by the work piece. This investigation will help to obtain more accurate temperature distribution profile and material removal rate. The formulation of the thermal model in this research has integrated the aspects of energy distribution factor, Gaussian heat distribution and latent heat of fusion to predict thermal behavior as well as material removal mechanism. In addition, this research Nitronic-30 is used as work piece material which is a novel aspect of this research work.

## 2. Literature review

Karidkar *et al* [1] proposed a thermal model to obtain accurate amount of material removed and temperature distribution profile. Banerjee *et al* [2] proposed a thermal model to calculate the temperature distribution in wire material to predict the wire failure as a result of thermal load. The model may help to prevent wire failure and better utilization of the process is obtained. Das *et al* [3] established a mathematical model to forecast cathode erosion in micro WEDM. It has been observed that the erosion rate is irrespective of wire velocity. Dekseyer *et al* [4] proposed a thermal model and reported that wire breakage frequency occurs frequently at sharp corners of the wire path by predicting thermal load on wire electrode.Van Djick *et al* [5] calculated the volume of molten metal using a heat conduction model and reported that the aspect of plasma channel widening should be considered in order to obtain more accurate results. Kalajahi *et al* [6] investigated the MRR using RSM and simulated the EDM process taking into account assumptions like plasma flushing efficiency, energy distribution factor temperature dependent material

*For correspondence
Published online: 08 April 2022

properties, Gaussian heat distribution and phase change so as to make the model more realistic. Joshi *et al* [7] have proposed a thermo-physical model using FEM and recommended energy distribution factor of 0.18-0.2 for medium energy zone and 0.18 for lower energy zone. Kansal *et al* [8] presented numerical solution of PMEDM using FEM. In this work, the material properties are varied with respect to temperature, it has been assumed that 9 % of the total heat is absorbed by the work piece, plasma flushing efficiency is assumed 20%, spark radius is considered 30-50% greater than that found. Saha *et al* [9] predicted the thermal distribution in the wire using FE (Finite Element) model in order to prevent wire breakage. The results showed that non-uniform heating is affecting the temperature and thermal strains in the wire material. Someh Habib *et al* [10] examined the effects of frequency of tungsten wire electrode and vibration amplitude during WEDM and showed that vibration amplitude decreases with decrease in wire tension. Vishwakarma *et al* [11] developed a single spark FE model to study the effect of MRR on MMC. The investigation revealed that the MRR is more in second discharge than the first because of high initial temperature of the work piece and occurrence of spark on crater ridge. Yeo *et al* [12] estimated the geometrical dimensions of micro-crater by considering the entire superheated area is ejected from the work-piece surface while only a small fraction of the molten area is expelled. From the literature review, it is noted that few researchers have addressed the WEDM process using finite element and simulation approach. Thus, to study the behavior of this thermoelectric process using appropriate software and assuming proper assumptions are of prime importance.

*Assumptions*

1. The model is developed for single spark.
2. The work-piece material and wire material is considered homogenous, isotropic.
3. The heat transfer takes place only through conduction.
4. The work piece geometry is axisymmetric about z- axis.
5. Gaussian heat source distribution is considered.
6. Plasma flushing efficiency is considered 100%.

## 3. Temperature model

### 3.1 *Governing equation*

Heating of work piece due to a single spark is governed by differential equation which is used by many researchers [1, 6–9, 11, 13–16] is given as follows,

$$\rho C \frac{\partial T}{\partial r} = \frac{1}{r} * \frac{\partial}{\partial r}\left(K * \frac{\partial T}{\partial r}\right) + \frac{\partial}{\partial z}\left(K * \frac{\partial T}{\partial z}\right) \quad (1)$$

### 3.2 *Heat distribution*

The accuracy of model depends on selection of appropriate heat source. When plasma channel incidents on the work piece surface, it causes temperature rise on the work piece surface. The plasma channel distribution may be of the distributed heat source or point heat source but in actual, these models are not realistic due to the fact that energy density of the spark radius varies with radius of plasma channel. In this work Gaussian heat distribution is considered which is more realistic and precise, also the Gaussian heat distribution is used by most of the researchers for modeling purpose [1, 6, 7, 11, 13–17].

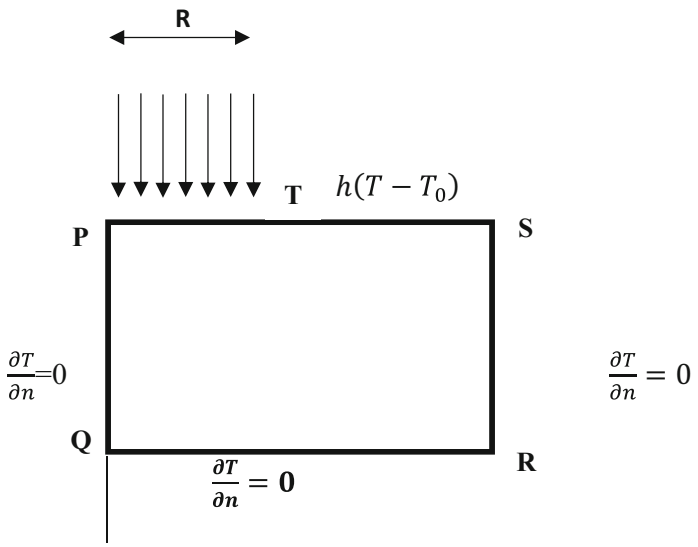


**Figure 1.** An axisymmetric thermal model.

### 3.3 *Boundary conditions*

Figure 1 shows the thermal model with boundary conditions.

From figure 1 it is clear that maximum heat flux is applied at point 'P' and minimum heat flux is applied towards the end of plasma radius 'R' at point 'T'. Therefore maximum temperature is applied at 'P' and minimum at point 'T'. Area PQRS is considered for thermal analysis. On the surface, PT heat is transferred due to Gaussian heat distribution and through conduction only. Beyond 'T' heat transfer takes due to convection. As SR and QR are away from the applied heat flux, no heat transfer is considered. For boundary PQ, the heat transfer is zero as it is an axis of symmetry [1]. Therefore the boundary conditions are:

1. $K\frac{\partial T}{\partial z} = Q(r)$……..for r<R for surface PS
2. $K\frac{\partial T}{\partial z} = hc(T - T_0)$……for r≥R for surface PS
3. $\frac{\partial T}{\partial n} = 0$……at boundary RS, QR & PQ.

### 3.4 *Heat flux*

The spark generated in the WEDM process follows Gaussian heat distribution and the heat flux is given by Kalajahi *et al* [6].

$$Q(r) = \frac{4.57F_C VI}{\pi R^2} * e^{-4.5\left(\frac{r^2}{R^2}\right)} \quad (2)$$

Where, Fc = Energy distribution factor

### 3.5 *Spark radius*

Spark radius (R) is a function of pulse on time and current which is calculated by using the equation given by

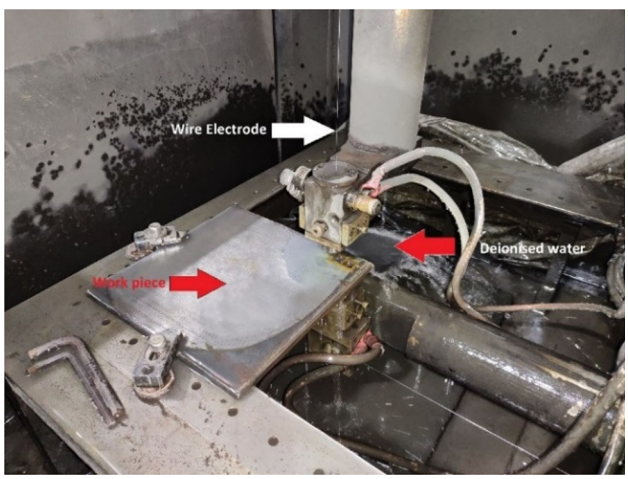


**Figure 2.** Experimental Setup.

$$R = \left(2.04 * I^{0.43} * Ton^{0.44}\right) \quad (3)$$

Shabgard *et al* [13]. Where, I = Peak current (Amp), Ton= pulse on time ($\mu$sec).

### 3.6 *Energy distribution factor*

Substantial amount of heat energy is discharged once the current is supplied, out of which small amount of energy which is absorbed by the work piece is partly utilized for melting and evaporation of the material and partly will be carried away by the dielectric fluid through convection. The energy distribution factor (Fc) is percentage of amount of energy absorbed by the work piece. Different researchers have proposed different values for Fc [6]. Different materials exhibit different values of Fc as the capability of material to absorb energy is different, therefore the value of Fc cannot be generalized (figure 2).

### 3.7 *Phase change*

The energy which is discharged during WEDM process generates sufficient amount of heat so that work piece is melted, vaporized consequently the latent heat during martensitic transformation and solidification. The increase in heat capacity because of this latent heat change during phase change can be incorporated in the form of an equation as given [6].

$$C_{Peff.} = C_p + \frac{CH}{\Delta T} \quad (4)$$

Where

CH (J/Kg) = latent heat of fusion

$$\Delta T = T_m - T_0$$

$T_m$ = Melting temperature of material

$T_0$ = Dielectric temperature at the beginning of machining process.

## 4. Experimentation

The experiments are performed on a CNC wire electric discharge machine of electronica supercut 704 for Nitronic-30 steel. Zinc coated brass wire of size 250 micron is used for the experimentation. The work piece thickness is 7.5 mm. The following figure shows the machining conditions.

The different controlled process parameters with their levels are given in the following table.

According to Taguchi, for 3 parameters and 3 levels, L9 array is selected and experiments are performed accordingly. The table shows levels of parameter for each experiment.

Experimental MRR is calculated using the equation,

$$\text{MRR} = \text{Kw} * \text{Mt} * \text{Vc} \tag{5}$$

Where, Kw = kerf width, Mt= Material thickness, Vc = Cutting speed.

## 5. Finite element modeling procedure

The following steps are employed for thermal modeling using ANSYS:

### 5.1 *Choice of element*

Two-dimensional quadrilateral axisymmetric model with size equal to 1mm*1mm is considered for each experiment.

### 5.2 *Defining material properties*

The material properties used are as follows,

Density ($\rho$) = $8100\,kg/m^3$

Specific heat (C) = 813 J/kg.k ….(Without latent heat)

Specific heat (C) = 1000 J/kg.k … (Considering latent heat)

Thermal conductivity (K) = 25.5 W/mk.

### 5.3 *Geometry*

In this step, an axisymmetric model of size 1mm*1mm is created and the mesh size = 1/10* plasma radius is considered.

### 5.4 *Heat flux calculation*

Heat flux on each element is computed by varying the radial distance. For node no.1, radial distance is zero, for node no. 2 it is equal 1/10* plasma radius and for node no.11 it is equal to plasma radius. As a result, the heat flux values for ten elements and for eleven nodes are obtained which covers the entire plasma radius.

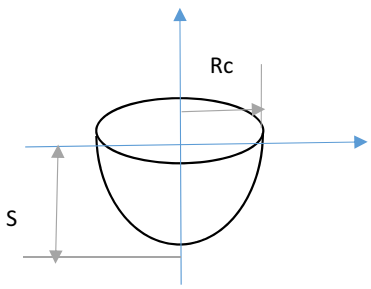


**Figure 3.** Geometry of the crater formed in single spark.

### 5.5 *Calculation of temperature on each node*

The temperature at each node is calculated using a formula given by Bejan [18] as follows:

$$T_f = T_i + \frac{Q}{\Delta z * \rho * C_p}\left[\frac{e^{-\frac{Uy^2}{4\alpha x}}}{(4\pi v \alpha x)^{0.5}}\right] \tag{6}$$

The temperature distribution profile is obtained by applying temperature to respective nodes on the work piece.

## 6. Determination of MRR from ANSYS

The elements which are having temperature greater than or equal to melting temperature of material are selected from the temperature distribution profile obtained from ANSYS. These elements are responsible for the material removal from work piece surface. Crater formed in single discharge are assumed to have circular parabolic geometry because the temperature distribution on the line PS & PQ are decreasing in nature and when the temperature profile is revolved about line PQ, it will produce a circular parabolic geometry and similar observations are reported by Shabgard *et al* [13], Vishwakarma *et al* [11] and Joshi *et al* [7] as shown in figure 3.

**Table 1.** Process parameters and their levels.

| Sl. no. | Parameter | Level 1 | Level 2 | Level 3 |
|---|---|---|---|---|
| 1 | Pulse on time (machine unit) | 110 | 115 | 120 |
| 2 | Pulse off time (machine unit) | 40 | 45 | 50 |
| 3 | Peak current (Amp) | 70 | 150 | 230 |

**Table 2.** Parameter levels for experimentation.

| | Parameter levels | | |
|---|---|---|---|
| Expt. No. | Pulse on time (machine unit) | Pulse off time (machine unit) | Peak current (Amp) |
| 1 | 110 | 40 | 70 |
| 2 | 110 | 45 | 150 |
| 3 | 110 | 50 | 230 |
| 4 | 115 | 40 | 230 |
| 5 | 115 | 45 | 70 |
| 6 | 115 | 50 | 150 |
| 7 | 120 | 40 | 150 |
| 8 | 120 | 45 | 230 |
| 9 | 120 | 50 | 70 |

**Table 3.** Expt. MRR.

| Experiment no. | Kw (mm) | Vc (mm/min) | Mt (mm) | MRR(Exp) ($mm^3$/min) |
|---|---|---|---|---|
| 1 | 0.273 | 2.86 | 7.5 | 5.85585 |
| 2 | 0.283 | 3.03 | 7.5 | 6.431175 |
| 3 | 0.291 | 2.31 | 7.5 | 5.041575 |
| 4 | 0.283 | 3.67 | 7.5 | 7.789575 |
| 5 | 0.286 | 4.09 | 7.5 | 8.77305 |
| 6 | 0.27 | 2.59 | 7.5 | 5.24475 |
| 7 | 0.273 | 2.99 | 7.5 | 6.122025 |
| 8 | 0.277 | 3.93 | 7.5 | 8.164575 |
| 9 | 0.276 | 4.2 | 7.5 | 8.694 |

Theoretical crater volume/pulse is given by,

$$Vc = \frac{1}{2} * \pi * S * Rc^2 \tag{7}$$

Where,

S= depth, $R_c$= Radius of crater.

Now, the total number of pulses can be calculated using the equation,

$$NOP = \frac{T_{machining}}{T_{on} + T_{off}} \tag{8}$$

Therefore, the theoretical MRR can be calculated as,

$$MRR = \frac{Vc * NOP}{T_{machining}} \tag{9}$$

The following tables shows the ANSYS MRR for each experiment (tables 1, 2, 3, 4 and 5).

## 7. Result

In this work, investigation is done by considering the effect of latent heat of fusion or phase change. As anticipated, the temperature is maximum at the beginning of spark radius where maximum heat flux is applied and gradually decreases as radial distance increases. The temperature distribution profile obtained is as shown in figure 4.

It is also evident from the results that, considering the latent heat of fusion results in reasonable agreement between experimental MRR and ANSYS MRR. The results obtained after applying the latent heat of fusion in the model are significantly closer to the experimental MRR as shown in figure 5.

**Table 4.** ANSYS MRR (without latent heat).

| Expt No. | S (micron) | Rc (Micron) | Vc($mm^3$) | T machining (Min) | Ton (MU) | Toff (MU) | No. of pulses | MRR ($mm^3$/min) |
|---|---|---|---|---|---|---|---|---|
| 1 | 8 | 30 | 1.13E-05 | 14.38 | 110 | 40 | 5.8E+06 | 4.5216 |
| 2 | 6 | 35 | 1.154E-05 | 14.41 | 110 | 45 | 5.6E+06 | 4.466903226 |
| 3 | 5 | 37 | 1.075E-05 | 18 | 110 | 50 | 6.8E+06 | 4.02999375 |
| 4 | 6 | 34 | 1.089E-05 | 11.47 | 115 | 40 | 4.4E+06 | 4.215298065 |
| 5 | 8 | 31 | 1.207E-05 | 10.14 | 115 | 45 | 3.8E+06 | 4.52631 |
| 6 | 8 | 31 | 1.207E-05 | 16 | 115 | 50 | 5.8E+06 | 4.389149091 |
| 7 | 9 | 29 | 1.188E-05 | 10.4 | 120 | 50 | 3.7E+06 | 4.194116471 |
| 8 | 8 | 39 | 1.91E-05 | 9.57 | 120 | 45 | 3.5E+06 | 6.946821818 |
| 9 | 7 | 38 | 1.587E-05 | 13.49 | 120 | 50 | 4.8E+06 | 5.601021176 |

**Table 5.** ANSYS MRR (with latent heat).

| Expt No. | S (micron) | Rc (Micron) | Vc($mm^3$) | T machining (Min) | Ton (MU) | Toff (MU) | No. of pulses | MRR ($mm^3$/min) |
|---|---|---|---|---|---|---|---|---|
| 1 | 8 | 35 | 1.539E-05 | 14.38 | 110 | 40 | 5.8E+06 | 6.1544 |
| 2 | 6.95 | 41 | 1.834E-05 | 14.41 | 110 | 45 | 5.6E+06 | 7.100218645 |
| 3 | 8 | 40 | 2.01E-05 | 18 | 110 | 50 | 6.8E+06 | 7.536 |
| 4 | 7 | 42 | 1.939E-05 | 11.47 | 115 | 40 | 4.4E+06 | 7.504397419 |
| 5 | 7 | 50 | 2.748E-05 | 10.14 | 115 | 45 | 3.8E+06 | 10.303125 |
| 6 | 9 | 35 | 1.731E-05 | 16 | 115 | 50 | 5.8E+06 | 6.294272727 |
| 7 | 9 | 37 | 1.934E-05 | 10.4 | 120 | 50 | 3.7E+06 | 6.827283529 |
| 8 | 7 | 51 | 2.858E-05 | 9.57 | 120 | 45 | 3.5E+06 | 10.39454182 |
| 9 | 9 | 46 | 2.99E-05 | 13.49 | 120 | 50 | 4.8E+06 | 10.55261647 |

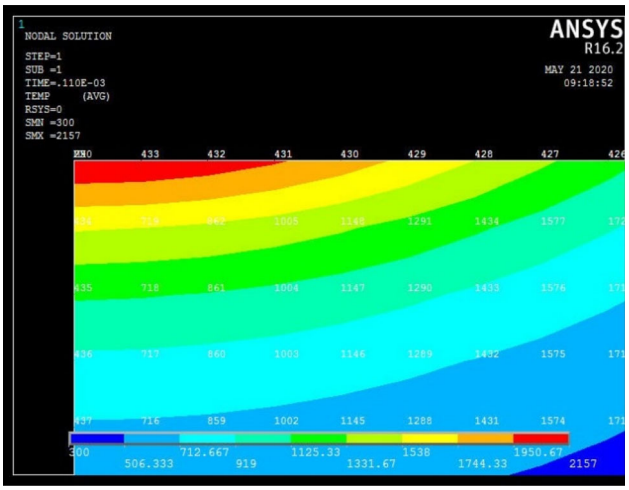


**Figure 4.** Temperature distribution profile for Ton=110 µs, Toff=45 µs and I=150 A.

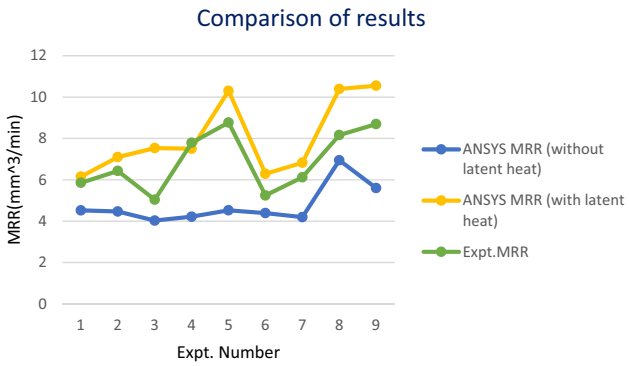


**Figure 5.** Comparison of experimental MRR with ANSYS MRR.

### 7.1 *Validation of results*

ANSYS MRR predicted by the proposed model is validated with experimental results. The ANSYS results show good agreement with experimental results with some variation. It is also seen from the results that, average % deviation from experimental MRR is about 30% without considering latent heat whereas it reduces to 18% when the effect of latent heat is considered. The deviation in the results may be because of the assumptions like 100% flushing efficiency, improper flushing of debris and no ignition delays which cannot be generalized into the model.

## 8. Conclusion

In this study, finite element thermal modeling for WEDM of Nitronic-30 steel is undertaken using finite element (ANSYS) software. The suggested model becomes more genuine and unique by introducing the effect of latent heat of fusion or phase change, calculating exact value of amount of energy absorbed by the work piece. This makes possible to develop more accurate and reliable model to predict accurate temperature distribution profile and helps to decide the material removal. The accuracy of the model can be further enhanced in future by considering the factors such as plasma flushing efficiency and ignition delays.

## References

[1] Karidkar S and Dabade U 2016 Finite Element Modeling and Simulation of Inconel 718 Using WEDM *ASME 2016 International Mechanical Engineering Congress and Exposition*

[2] Banerjee S, Prasad B and Mishra P 1993 A simple model to estimate the thermal loads on an EDM wire electrode. *Journal of Materials Processing Technology.* 39: 305–317

[3] Das S and Joshi S 2010 Modeling of spark erosion rate in microwire-EDM. *The International Journal of Advanced Manufacturing Technology.* 48: 581–596

[4] Dekeyser W, Snoeys R and Jennes M 1988 Expert system for wire cutting EDM, based on pulse classification and thermal modeling. *Robotics and Computer-Integrated Manufacturing.* 4: 219–224

[5] Van Dijck F and Dutre W 1974 Heat conduction model for the calculation of the volume of molten metal in electric discharges. *Journal of Physics D: Applied Physics.* 7: 899–910

[6] Kalajahi M, Ahmadi S and Oliaei S 2013 Experimental and finite element analysis of EDM process and investigation of material removal rate by response surface methodology. *The International Journal of Advanced Manufacturing Technology.* 69: 687–704

[7] Joshi S and Pande S 2010 Thermo-physical modeling of die-sinking EDM process. *Journal of Manufacturing Processes.* 12: 45–56

[8] Kansal H, Singh S and Kumar P 2008 Numerical simulation of powder mixed electric discharge machining (PMEDM) using finite element method. *Mathematical and Computer Modelling.* 47: 1217–1237

[9] Saha S, Pachon M, Ghoshal A and Schulz M 2004 Finite element modeling and optimization to prevent wire breakage in electro-discharge machining. *Mechanics Research Communications.* 31: 451–463

[10] Habib S and Okada A 2016 Study on the movement of wire electrode during fine wire electrical discharge machining process. *Journal of Materials Processing Technology.* 227: 147–152

[11] Vishwakarma U, Dvivedi A and Kumar P 2012 FEA modeling of material removal rate in electrical discharge machining of Al6063/SiC composites *International Journal of Mechanical and Aerospace Engineering*.6: 398–403

[12] Yeo S, Kurnia W and Tan P 2007 Electro-thermal modelling of anode and cathode in micro-EDM. *Journal of Physics D: Applied Physics.* 40: 2513

[13] Shabgard M, Seyedzavvar M, Oliaei S and Ivanov A 2011 A numerical method for predicting depth of heat affected zone

in EDM process for AISI H13 tool steel. *Journal of Scientific and Industrial Research.* 70: 493–499

[14] Mohapatra K 2016 Thermal Modeling and Structural Analysis in wire EDM Process for a 3D model. *Applied Mechanics and Materials.* 852: 279–289

[15] Singh M 2018 Thermal simulation of machining of alumina with wire electrical discharge. *Journal of Mechanical Science and Technology.* 32: 333–343

[16] Kumar J 2020 Three-Dimensional Numerical Modelling of Temperature Profiles on theWire Electrode During Wire Electric Discharge Machining Process In: *International Conference on Recent Innovations and Developments in Mechanical Engineering, Meghalaya*

[17] Das S and Joshi S 2018 Thermal Modeling and Simulation In: *Proceedings of All India Manufacturing Technology, Design and Research* 120-135

[18] Bejan A 2013 *Heat transfer*. 3rd edn. John Wiley & Sons Inc, New York